Eur. Phys. J. A **29**, 175–182 (2006)
DOI 10.1140/epja/i2006-10074-0

THE EUROPEAN PHYSICAL JOURNAL A

Beta decay of ^{94}Pd and of the 71 s isomer of ^{94}Rh

L. Batist[1,2,a], A. Blazhev[3,4], J. Döring[4], H. Grawe[3], M. Kavatsyuk[3,5], O. Kavatsyuk[3,5], R. Kirchner[3], M. La Commara[2], C. Mazzocchi[3], I. Mukha[3,6], C. Plettner[3], E. Roeckl[3], and M. Romoli[2]

[1] St. Petersburg Nuclear Physics Institute, RU-188350 Gatchina, Russia
[2] Department of Physics of the University "Federico II", and INFN-Napoli, I-80126 Napoli, Italy
[3] Gesellschaft für Schwerionenforschung, D-64291 Darmstadt, Germany
[4] University of Sofia, BG-1164, Sofia, Bulgaria
[5] National Taras Shevchenko University of Kyiv, 01033 Kyiv, Ukraine
[6] University of Seville, E-41012 Sevilla, Spain

Received: 19 April 2006 / Revised: 29 June 2006 /
Published online: 29 August 2006 –
Communicated by J. Äystö

Abstract. The β decay of ^{94}Pd and of the 71 s isomer of ^{94}Rh was investigated by using total γ-ray absorption techniques. Several levels in ^{94}Rh are established, including a new low-lying isomer characterized by a half-life of 0.48(3) μs and a de-exciting transition of 55 keV. $E2$ multipolarity is determined for this transition by measuring the intensities of its γ-rays and the characteristic X-rays from its electron conversion. On the basis of the measured reduced β-decay transition rates to known ^{94}Ru levels and shell model considerations, the spin-parity of the 71 s and the 0.48 μs isomers of ^{94}Rh is assigned to be (4^+) and (2^+), respectively. The β-decay strength distributions measured for ^{94}Pd and the 71 s isomer of ^{94}Rh yield $Q_{\rm EC}$ values of 6700(320) and 9750(320) keV for these decays and give evidence for the population of those states below and above the magic $N = 50$ gap that belong to both components of the $0g$ spin-orbit doublet.

PACS. 27.60.+j $90 \leq A \leq 140$ – 21.10.Hw Spin, parity, and isobaric spin – 21.10.Tg Lifetimes – 23.40.-s Beta decay; double beta decay; electron and muon capture

1 Introduction

Studies of nuclei near the $N = Z = 50$ shell closure at ^{100}Sn offer a rich source of nuclear-structure information on medium-mass nuclei. In addition to in-beam spectroscopy, decay studies represent a valuable tool, including investigations of β decay as well as direct charged-particle radioactivity [1]. The direct one-proton [2] and two-proton [3] disintegration of the (21^+) isomer of ^{94}Ag is a particularly exciting recent example of such studies of exotic nuclei. In addition to their nuclear-structure interest, studies of $A > 64$, $N \approx Z$ nuclei are also relevant for modeling the path of the astrophysical rp-process [4] in general, and the recently proposed νp-process [5] in particular.

Among the nuclei which lie on the nuclear chart "southeast" of ^{100}Sn, whose $0g_{9/2}$ orbital is partly or completely filled and which are accessible to experimental investigations, the odd-odd nucleus ^{94}Rh ($Z = 45$, $N = 49$) is one of the least investigated. According to the NUBASE evaluation [6], two long-lived states have been identified for this nucleus, their half-lives being 70.6(6) and 25.8(2) s, respectively. It is not clear, however, which of the two states, which we shall denote by ^{94m1}Rh and ^{94m2}Rh, respectively, represents the ground state. While a tentative spin and parity assignment of (8^+) is given for ^{94m2}Rh [6], the corresponding properties of ^{94m1}Rh are rather uncertain. Very little is known on the β^+/EC decay of ^{94}Pd as only its half-life ($T_{1/2} = 9.0(5)$ s [6]) and a few β-delayed γ-rays were measured, without a decay scheme being established [7]. Moreover, it was observed that a β-delayed γ transition populates ^{94m1}Rh. However, the β-decay data taken so far do not allow one to clarify the spin and parity assignment of ^{94m1}Rh. As its β decay strongly feeds 2^+ and 4^+ states in ^{94}Ru, a spin-parity of 3^+ was suggested for this isomer [8]. In contrast, a theoretical investigation of the β decay of $N = 49$ nuclei by Johnstone and Skouras [9] revealed a severe disagreement between the experimental half-life value of 71 s and the corresponding prediction based on the 3^+ assignment. The calculation also failed to reproduce the low energy of a 3^+ state, but at the same time predicted the first two excited states of ^{94}Rh to be almost degenerate 2^+ and 4^+ levels. Johnstone

[a] e-mail: batist@pnpi.spb.ru

and Skouras [9] explained these discrepancies by assuming that the 71 s decay represents a mixture of β decays of the 2^+ and 4^+ levels. Herndl and Brown [10] assigned 4^+ to ^{94m1}Rh in their wide-range shell model calculations of the half-lives of $(1p_{1/2}, 0g_{9/2})$ nuclei.

The previous assignment of spin-parity 3^+ to ^{94m1}Rh [8] as well as the theoretical consideration [9] were based on the experimental β-decay feedings to the ^{94}Ru states which have reliably established spin-parity assignments. However, these feedings were determined from a balance of γ-ray intensities and hence represent "apparent feedings" ($I_{\rm app}$) which may differ from the true β feedings (I_β). The latter shortcoming is due to the fact that a sizeable fraction of the γ-ray intensity coming from high-lying excited states may easily remain unobserved because of a very fragmented character of the γ-ray de-excitation, known as the Pandemonium problem [11]. This leads to an underestimation of I_β for high-lying daughter states, and consequently to its overestimation for low-lying daughter states. Therefore, in order to solve the ambiguity of the spin-parity assignment of ^{94m1}Rh, the true β feeding to ^{94}Ru states has to be measured. Based on this motivation, we re-investigated the ^{94m1}Rh decay by using the total absorption spectrometer (TAS) [12] that is able to detect whole γ-ray cascades rather than individual γ transitions.

The application of the TAS for the β^+/EC-decay study of the nuclei under consideration here is expected to give new data on the corresponding Gamow-Teller (GT) strengths. The investigations of very neutron-deficient nuclei near ^{100}Sn with $Z \leq 50$ and $N \geq 50$ performed with both, the high-resolution technique [13] and TAS [14–18] have revealed strong feeding of high-lying daughter states. In the framework of the shell model consideration, such decay is due to a GT spin-flip (SF) [19] transformation of a proton in the partly or completely filled $0g_{9/2}$ orbit into a neutron in the $0g_{7/2}$ orbit. It is important that the main GT strength is situated within the $Q_{\rm EC}$ window which makes the entire GT strength available to β-decay studies. In nuclei with $Z, N < 50$ the GT transformations $\pi(g_{9/2}) \rightarrow \nu(g_{9/2})$ which are responsible for the β decay to low-lying daughter states, become available. In analogy to charge-exchange reactions [19] we will use the denotation "core-polarized" (CP) for these states. (There should not be confusion with the denotation "core polarisation" referring one of the effects leading to quenching of GT strength.) The SF excitations are not expected to be affected by the opening of the CP transformation channel. Therefore one expects the β decay to populate two groups of excited states, separated by an energy interval depending on the spin-orbit splitting of the $0g$ orbit. This expectation is also supported by the observation of strong branching ratios for β-delayed proton emission in the decay of the light silver isotopes, ^{96}Ag [20] and ^{94}Ag [21].

This paper is organized as follows. In sect. 2, a short description of the experimental technique and the experimental results is given. Section 3 is devoted to the treatment of the experimental data, including in particular the identification of a new isomer in ^{94}Rh denoted by ^{94m3}Rh and the method of deducing the distribution of I_β, as well as the $Q_{\rm EC}$ values of ^{94}Pd and ^{94m1}Rh. In sect. 4, the spin-parity assignment of ^{94m1}Rh and ^{94m3}Rh will be discussed as resulting from these data, and the experimental GT-strength distributions will be presented. The theoretical estimates used during the analysis were calculated in the shell model framework with the code OXBASH [22] in a $(1p_{1/2}, 0g_{9/2})$ model space. Section 5 contains the summary and the conclusions.

2 Experimental techniques

^{94}Pd nuclei were produced through fusion-evaporation reactions induced by a $4.8\,A \cdot$ MeV ^{40}Ca beam on a ^{58}Ni target. The recoils were stopped in the graphite catcher of a FEBIAD ion source [23]. The ^{94}Pd beam from the GSI on-line mass separator [24], whose intensity amounted to 12 atom/s, was implanted into a movable tape which transported the radioactive sources into the centre of the TAS [12]. The TAS consists of a large NaI crystal with 356 mm length and 356 mm diameter, with ancillary germanium (Ge) and silicon (Si) detectors positioned near the centre of the NaI crystal. The Ge detector offers the possibility to record X- and γ-rays from sources positioned in the centre of the TAS, with the NaI crystal and its lead shielding efficiently suppressing the room background. By using appropriate coincidence conditions with signals from these ancillary detectors, the events related to β^+ and EC decay can be distinguished. In the following, the spectra registered in the NaI detector in prompt coincidence with one of the two Si detectors or characteristic Rh or Ru X-rays are denoted as TAS(β^+) and TAS(EC), respectively.

The TAS(β^+) spectra of the ^{94}Pd and ^{94m1}Rh were produced in sufficient isotopic purity due to the low intensity of the mass-separated ^{94}Ag beam [25] and by choosing an appropriate timing of the implantation measurement cycle. As the yield of short-lived rhodium isotopes from the FEBIAD ion source is suppressed due to the poor diffusion and surface release properties of this element, the mass-separated $A = 94$ beam contains only minor amounts of ^{94m1}Rh and ^{94m2}Rh. However, we were able to produce sufficiently strong samples of ^{94m1}Rh activity as a daughter of ^{94}Pd β decay. In order to obtain data sets for the 9 s ^{94}Pd and 71 s ^{94m1}Rh activities, two different implantation measurement cycles were used, whose timing was 24 s - 24 s and 64 s - 64 s, respectively. The total number of cycles amounted to 1200 and 150, corresponding to measurement times of about 8 and 3 h, respectively. The time dependence of the total TAS(β^+) spectra as a function of time after the completion of the source transport was analysed using two half-life components. The best fit to the experimental data was obtained with values of 9.6(2) and 66(6) s, which agrees with the results from previous measurements for the half-life of ^{94}Pd and ^{94m1}Rh [6], respectively. The contribution of the 52 min ^{94}Ru component to the TAS spectra was neglected.

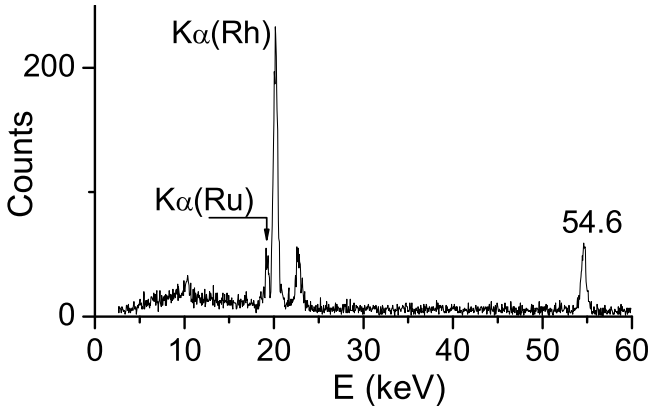

Fig. 1. Low-energy part of a spectrum registered by the Ge detector during measurement with 24 s cycles.

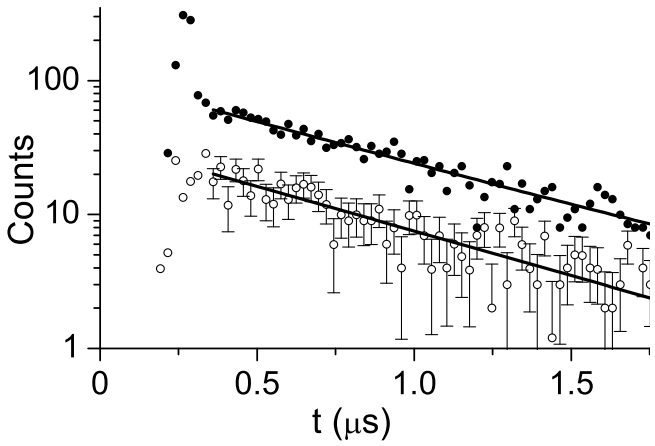

Fig. 2. Time distribution of events obtained as K_α(Rh)γNaI (filled circles) and γ(55 keV)γNaI (open circles) coincidences.

3 Experimental results

3.1 Identification of ^{94m3}Rh

The spectrum registered by the Ge detector for the 24 s cycle is displayed in fig. 1. Peaks corresponding to the characteristic Ru and Rh X-rays and γ-rays with an energy of 54.6 keV were observed in this spectrum. This β-delayed γ-ray has already been reported earlier [7]. The intensities of K_α(Rh) X-rays and 55 keV γ-rays were found to decrease with a half-life of 9.6(7) and 11(2) s, respectively, in agreement with the half-life of the ^{94}Pd component determined using the decomposition of TAS(β^+) spectra (see sect. 2).

The time distribution of delayed-coincidence events, produced by registering the time of 55 keV γ-ray events relative to the time of γ-ray events in the NaI detector shown in fig. 2, yields a half-life 0.45(3) μs. The corresponding time distribution of K_α (Rh) X-rays shown in the same figure contains both the prompt and delayed components, the half-life of the latter being 0.50(2) μs in agreement with that of the 55 keV γ-rays. We thus assign the 55 keV γ-ray to represent the γ-ray transition deexciting of a new isomer ^{94m3}Rh while the delayed component of the X-ray is due to the internal electron conversion of this transition. The half-life of ^{94m3}Rh was evaluated to be 0.48(3) μs. By using the ratio of the intensities of delayed K_α(Rh) X-rays and 55 keV γ-rays, the internal conversion coefficient of the 55 keV transition was evaluated to be $\alpha_K = 9.5(20)$. Within the limits of its experimental uncertainty this value is consistent with the theoretical α_K value for an $E2$ transition and with a theoretical upper limit of 0.2 for the $M1/E2$ ratio [26]. The summed intensity of delayed X-rays and 55 keV γ-rays was measured to be close to 100% with an uncertainty of about 20%. This observation means that most of β-delayed γ-rays populate the 0.48 μs isomer ^{94m3}Rh.

3.2 TAS spectra of ^{94}Pd and ^{94m1}Rh

The TAS spectra of ^{94}Pd and ^{94m1}Rh are shown in figs. 3 and 4, respectively. The energy positions of peaks in TAS(β^+) spectra are shifted by 1.022 MeV due to absorption of the annihilation quanta. The EC events of the ^{94}Pd decay were selected by using the prompt component of K_α (Rh) X-rays. In the TAS spectra of ^{94}Pd, a prominent peak at 558 keV appears, confirming the previous observation [7], as well as three more rather pronounced peaks. In the TAS(β^+) spectrum of the ^{94m1}Rh decay, three peaks corresponding to the known low-lying levels in ^{94}Ru are clearly observed.

The EC branching ratio was evaluated to be EC = 0.09(2) and EC = 0.16(4) for the ^{94}Pd and ^{94m1}Rh decay, respectively. In spite of their poor counting statistics, the TAS(EC) and TAS(β^+) spectra shown in fig. 3 agree as far as their overall structure and the most intense peaks are concerned. An exception is the 2570 keV peak in the

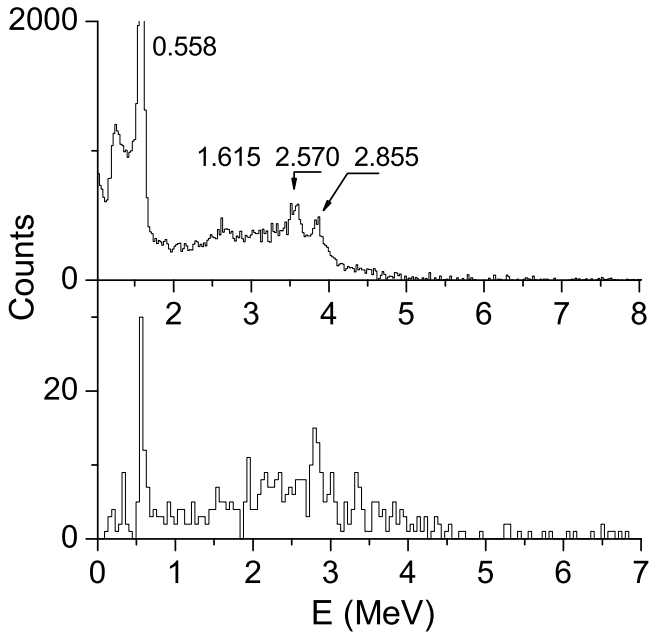

Fig. 3. Total absorption spectra of ^{94}Pd decay registered in coincidence with positrons (upper panel) and the fast component of K_α(Rh) X-rays (lower panel).

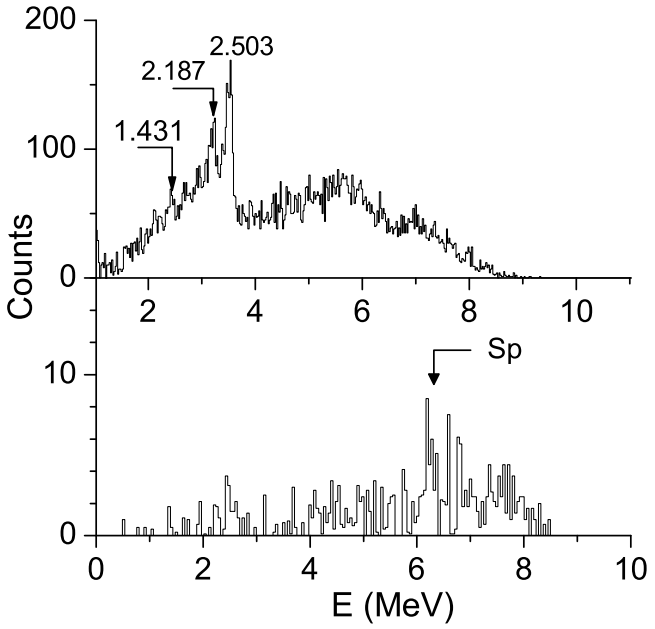

Fig. 4. Total absorption spectra of ^{94m1}Rh decay registered in coincidence with positrons (upper panel) and K_α(Ru) X-rays (lower panel). The literature value of the proton separation energy in ^{94}Ru is indicated.

TAS(β^+) spectrum of ^{94}Pd that is not observed in the TAS(EC) spectrum taken in prompt K_α(Rh) X-ray coincidence. By comparing with the intensity of the 2570 keV peak occurring in the TAS(β^+) spectrum, the corresponding peak in the TAS(EC) spectrum is expected to contain 15(7) events. Therefore, the non-observation of the latter peak may simply be due to the low counting statistics. Anyway the assignment of the 2570 keV peak in the TAS(β^+) spectrum to the β^+ decay of ^{94}Pd is firm as the same peak occurs in the TAS(β^+) spectrum accumulated in delayed coincidence with K_α(Rh) X-rays. The latter spectrum is caused by β^+-delayed γ-rays populating the 0.48 μs isomer ^{94m3}Rh. In principle, the disappearance of the EC component of a β-delayed ^{94}Rh transition could mean a high β-decay energy, which would suggest a decay of an isomeric state in ^{94}Pd at an energy of several hundred keV. This explanation, however, seems to be far fetched because such a long-lived isomeric state is not expected in an even-even nucleus. Note that for both ^{94}Pd and ^{94m1}Rh the present study exceeds by far the excitation energies in the daughter nuclei ^{94}Rh and ^{94}Ru that were attained in previous β-decay studies.

3.3 Beta-intensity distributions

The intensities of β^+ and EC decay (I_β) have been evaluated using a technique described in [18]. The essence of the method is the fitting of the experimental spectra by simulated ones. The simulation of a spectrum is definite if the level scheme and the γ branching ratios of the daughter nucleus are known to some extent. As this condition was not fulfilled for the daughter of the ^{94}Pd β decay, ^{94}Rh, a statistical assumption with respect to the structure of the γ cascades had to be made. Following [18], the daughter levels required for the simulation of the β-delayed γ-ray cascades were calculated in the shell model framework. The calculation were carried out in the $(1p_{1/2}, 0g_{9/2})$ model space with empirical interaction S-FIT [27] that was obtained by fitting levels of $N = 49$, 50 nuclei and should thus be particularly suited to reproduce the low-lying ^{94}Rh states. These states do not reproduce all the states that were expected to be fed in β decay but is quite sufficient for the statistical simulation of their γ decay. Tables 1 and 2 compile the I_β and log ft values for the ^{94}Pd and ^{94m1}Rh decay, respectively, as deduced from the peaks in the TAS spectra.

The excitation energies of ^{94}Rh levels, listed in table 1, are given relative to that of ^{94m1}Rh. By assuming that most of β-delayed γ-rays populate the 0.48 μs isomer ^{94m3}Rh (see sect. 3.1), these energies were obtained by increasing the energies determined for the peaks in the TAS spectra by 55 keV. The energy of the most strongly populated level at 613 keV was deduced by using the energy

Table 1. Levels in ^{94}Rh observed in ^{94}Pd β decay; feeding intensities I_β, log ft, and reduced probabilities B(GT).

Energy (MeV)	I^π	I_β(%)	log ft	B(GT)
0.0	(4^+)	< 1		
0.0546[a]	(2^+)	< 1		
0.613	(1^+)	42(5)	4.75	0.068(8)[b]
1.67(1)	(1^+)	3.9(7)	5.32	0.019(4)[b]
2.63(1)	(1^+)	10(2)	4.44	0.14(3)[b]
2.91(1)	(1^+)	15(3)	4.07	0.33(7)[b]
1.4–5.0		58[c]	3.33[c]	1.80(40)[b]
Total		$\equiv 100$	3.31	1.86(40)[b]

[a] $t_{1/2} = 0.48(3)\,\mu$s, $\alpha K = 9.5(20)$.
[b] Uncertainty owing to $Q_{\rm EC}$ not included.
[c] I_β and B(GT) of the levels 1.67, 2.63 and 2.91 MeV included.

Table 2. Characteristics of feeding to ^{94}Ru states in ^{94m1}Rh β decay; feeding intensities I_β, log ft and reduced probabilities B(GT).

Energy (MeV)	I^π	I_β(%)	log ft	B(GT)
0.0	0^+	< 1		
1.431[a]	2^+	< 1		
2.187[a]	(4^+)	4.3(15)	7.1	0.00032(12)[b]
2.498[a]	(6^+)	< 3		
2.503[a]	(4^+)	17.3(20)	6.4	0.0015(2)[b]
2.5–3.0		< 2		
3.0–9.0		≈ 75	3.8[c]	0.64[b,c]
Total		$\equiv 100$	3.35	1.06(20)[b,d]

[a] Data from [8,28].
[b] Uncertainty owing to $Q_{\rm EC}$ not included.
[c] Only $\beta\gamma$ decay.
[d] Including βp decay [7] at excitation energy lower than 9.0 MeV.

of 558.2 keV γ transition from [7]. No information concerning the γ de-excitation of the other ^{94}Rh levels can be derived from the TAS data. In particular, the question related to the 723.9 and 797.8 keV γ-transitions observed in [7] remains still open.

The excitation energies of ^{94}Ru levels listed in table 2 were taken from [8,28]. The I_β values obtained for the ^{94m1}Rh decay in our work differ from those published previously. The main difference concerns the 2_1^+ level at 1431 keV for which we found only an upper I_β limit of 1%, while the $I_{\rm app}$ value (see sect. 1) amounts to 18% [8]. The observation of a weak 1431 keV peak in the TAS(β^+) spectrum shown in fig. 4 is interpreted as being due to the fact that strong high-energy γ transitions feeding this level partly escape the TAS detection. This interpretation is supported by a simulation that takes into account the strong β feeding observed for high-lying ^{94}Ru states (see fig. 4). Our data indicate strong β feeding of 17% for the ^{94}Ru level at 2498 and/or 2503 keV. The corresponding $I_{\rm app}$ values determined in [8] amount to 7% and 31%, respectively. Therefore, the I_β result from our work is to be mainly attributed to the 4_2^+ level at 2503 keV. In total the ^{94}Ru levels in the energy region below 3 MeV are populated by only about 25% of the total β intensity of the ^{94m1}Rh decay. The main part of the β feeding apparently populates higher-lying ^{94}Ru levels, an observation that was missed in the previous study [8].

3.4 $Q_{\rm EC}$ values of ^{94}Pd and ^{94m1}Rh

During the simulation presented in sect. 3.3, we used the method described in [18] to estimate $Q_{\rm EC}$ values on the basis of experimental β^+/EC ratios. The results are 6700(320) and 9750(320) keV for ^{94}Pd and ^{94m1}Rh, respectively. The large uncertainties are mainly related to the low counting statistics. The $Q_{\rm EC}$ values obtained in this work agree with the results of 6590(600) and 9632(450) keV derived in the most recent mass compilation [29]. It is interesting to note that this compilation gives the excitation energy of ^{94m2}Rh as 320(200) keV relative to that of ^{94m1}Rh [6,29]. Moreover, the $Q_{\rm EC}$ value of ^{94m1}Rh, obtained in our work, agrees with the result of about of 9650 keV that can be extracted for the ^{94}Rh mass by using the data mapped in fig. 1 of [30]. Using this figure, we estimated the uncertainty of the above-mentioned value to be less than 20 keV. As the nuclei investigated in [30] were produced in a fusion-evaporation reaction, most probably the mass value found in this work pertains to the (8^+) isomer ^{94m2}Rh. If we thus assign the $Q_{\rm EC}$ value of 9650 keV from [30] to the (8^+) isomer ^{94m2}Rh, its excitation energy is 100(320) keV lower than that of ^{94m1}Rh. This sequence of ^{94m1}Rh and ^{94m2}Rh is hence opposite to that predicted by extrapolating systematic trends [6, 29], even though the energy difference obtained by the two methods agrees within the respective uncertainties. All in all, in spite of the high accuracy of the measurement reported in [30], hereinafter we used the $Q_{\rm EC}$ values obtained in our work for determining the statistical rate function of β decay (f) for both ^{94}Pd and ^{94m1}Rh.

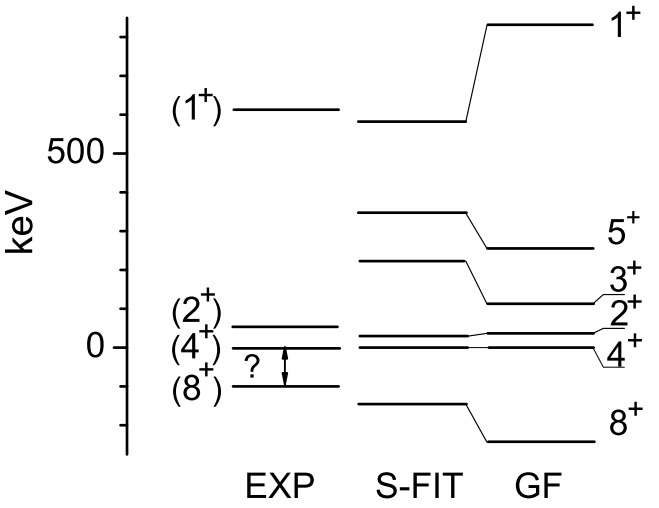

Fig. 5. Shell model predictions for low-lying ^{94}Rh levels in comparison with the corresponding experimental data. There is an indication from experiment that the position of the (8^+) state is 100(300) keV below the (4^+) state (see text).

4 Discussion

4.1 Spin and parity of ^{94m1}Rh and ^{94m3}Rh

Our data presented in table 2 show the β feeding to the ^{94}Rh levels at 2187 and 2503 keV whose spin and parity were previously assigned as 4^+ [8,28], but do not confirm the strong feeding to the 2_1^+ level in ^{94}Ru. This allows us to confirm the objection of Johnstone and Skouras [9] against the assignment of 3^+ to ^{94m1}Rh (see sect. 1). Therefore, following the works [9,10], we tentatively assign a spin-parity of 4^+ to ^{94m1}Rh. The possibility of the spin-parity assignment 5^+ is rejected as the shell model calculations persistently put this state above the 4^+ level, as shown in fig. 5. The positions of the ^{94}Rh levels shown in the figure were calculated using the $(1p_{1/2}, 0g_{9/2})$ model space with two different empirical interactions, namely S-FIT [27] and the interaction introduced by Gross-Frenkel (GF) [31].

The shell-model calculations predict that the low-lying 2^+ and 3^+ states can be considered as candidates for the 0.48 μs isomer ^{94m3}Rh. Making use of the wave functions calculated within the $(1p_{1/2}, 0g_{9/2})$ model space and employing the GF interaction, we estimated that the $3^+ \rightarrow 4^+$ transition with an experimental energy of 55 keV should be faster than 0.01 ns, with a strong dominance of the $M1$ component. This contradicts both the experimental result of 0.48 μs and the experimental upper limit of 0.2 for the $M1/E2$ ratio (see sect. 3.1). The contradiction cannot be eliminated by varying within reasonable limits the effective charges of $e_p = 1.72e$ and $e_n = 1.44e$ [32] and the effective g-factors, which were taken as their free-nucleon values. In contrast, the shell model calculation yields a half-life of 0.57 μs for the $2^+ \rightarrow 4^+$ $E2$ transition in satisfactory agreement with experiment. Therefore, we tentatively assign 2^+ to the 0.48 μs level. This conclusion is supported by the fact that shell model calculations

"prefer" the 2^+ rather than 3^+ assignment for the second excited ^{94}Rh level as can be seen in fig. 5.

4.2 Gamow-Teller strength distributions of ^{94}Pd and ^{94m1}Rh

The distributions of the β strength in the daughter nuclei ^{94}Rh and ^{94}Ru are displayed in the fig. 6 and fig. 7, respectively. In these figures and in tables 1 and 2 we designate the reduced probability as B(GT) for individual levels and for the unresolved continuum distribution. In the latter case the reduced probability is related to energy intervals of 200 keV. The B(GT) values are given in units of $g_{\rm A}^2/4\pi$ with the axial vector coupling constant $g_{\rm A} = 1.263\, g_{\rm V}$. For the ^{94m1}Rh decay, the contribution from β-delayed protons, whose intensity was determined in [7], has been taken into account. This was done by assuming the proton separation energy of 6254 keV [29] and the emission of all protons to the ground state of ^{93}Tc. The very large uncertainties of the $Q_{\rm EC}$ values (see sect. 3.4) induce correspondingly large B(GT) uncertainties whose relative values go up to 50%. Therefore, the following consideration is of rather qualitative nature. Considering, in particular, the ^{94m1}Rh decay, the used distribution of β-delayed protons gives a divergence of evaluated strength near $Q_{\rm EC}$. This effect could be eliminated by increasing the $Q_{\rm EC}$ of ^{94m1}Rh slightly, *i.e.* within its uncertainty. However, as only a few events have been observed [7] in the corresponding high-energy region of the β-delayed proton spectrum, such an adjustment does not seem to be justified.

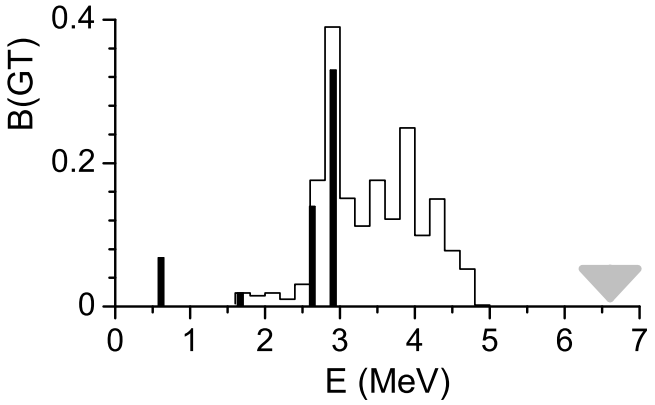

Fig. 6. GT-strength distribution for the decay of ^{94}Pd. The B(GT) values are given for 200 keV intervals. The filled bars indicate the B(GT) for the individual resolved levels. The excitation energy is given relatively to that of ^{94m1}Rh. The triangle indicates the $Q_{\rm EC}$ value of ^{94}Pd determined in this work.

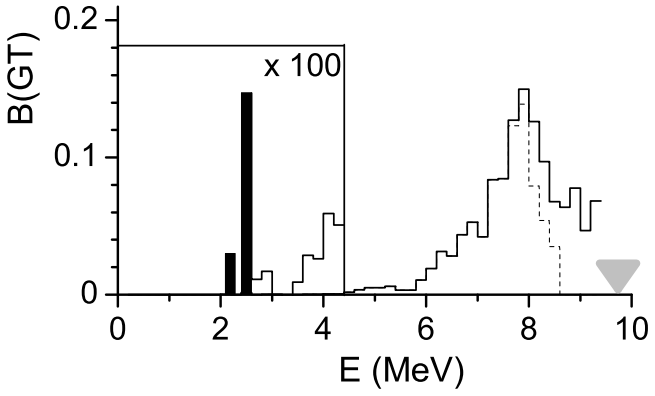

Fig. 7. GT-strength distribution for the decay of ^{94m1}Rh. The B(GT) values are given for 200 keV intervals. The filled bars indicate the B(GT) for the individual resolved levels. The dashed line shows the B(GT) distribution obtained by disregarding β-delayed proton emission. The triangle indicates the $Q_{\rm EC}$ value of ^{94m1}Rh determined in this work.

For the decays under consideration here, the GT strength is expected to originate mainly from the transformation of both CP-type $\pi(g_{9/2}) \rightarrow \nu(g_{9/2})$ and SF-type $\pi(g_{9/2}) \rightarrow \nu(g_{7/2})$, the former leads to the feeding to low-energy levels, while the latter can be suggested to be responsible for a wide resonance at higher excitation energy. The experimental summed B(GT) values are substantially larger than the shell model estimates of the CP component of GT strength. The shell model calculation within the $(1p_{1/2}, 0g_{9/2})$ model space with S-FIT ineraction yields values of 0.15 and 0.024 for the summed GT strength of the ^{94}Pd and ^{94m1}Rh decays, respectively, an universal hindrance factor $h = 1.6$ included [33]. Yet the experimental summed B(GT) for the β decay of ^{96}Pd, for which the SF transformation $\pi(g_{9/2}) \rightarrow \nu(g_{7/2})$ is expected to dominate owing to the completely filled neutron $0g_{9/2}$ shell, was measured to be 2.3 [34]. This value, used as estimate, allows referring the wide resonances in figs. 6, 7 to the SF mode.

For the ^{94}Pd decay, an independent confirmation of the SF nature of the high-energy GT excitation follows from the comparison of the centroid of the high-energy component of the GT strength in ^{94}Rh with the corresponding results for ^{96}Rh and ^{98}Rh as it is shown in fig. 8. The latter data were obtained by evaluating experimental observations made for the β decay of ^{96}Pd [34] and ^{98}Pd [35]. For these two nuclei, as it was pointed above, the SF transfor-

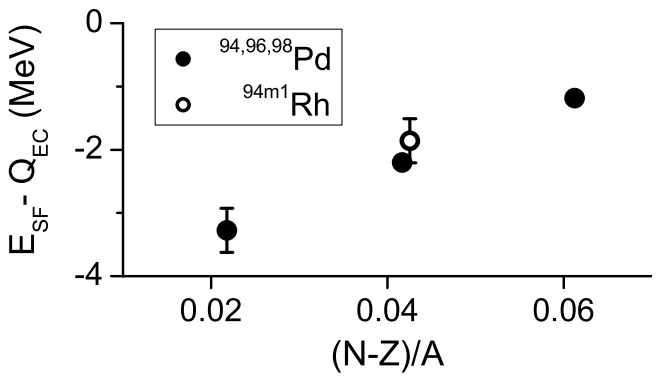

Fig. 8. Energies of the SF centroids of the GT-strength distribution with respect to the ground states of the parent nuclei. The position of $E_{\rm SF}$ for ^{94m1}Rh decay is shifted by 0.1 MeV to take into account the difference of Coulomb displacement energies [36] between ^{94}Rh and ^{96}Pd.

mation $\pi(g_{9/2}) \rightarrow \nu(g_{7/2})$ is expected to dominate. The calculations of Brown and Rykaczewski [13] and that of Johnstone [37] indicate that the ^{96}Pd β-decay strength is fully collected within the $Q_{\rm EC}$ window. Correspondingly, the centroid of the experimental B(GT) distribution of ^{96}Rh should be close to the centroid $E_{\rm SF}$ of the total GT strength. The energy scale used in fig. 8 reflects the nature of the SF-GT excitation as a $(I^{\pi}, T) = (1^{+}, 1)$ particle-hole pair added to the ground state of the parent nucleus. Following to [38], in order to analyse the energies of GT excitation in nuclei with different Z, the energies of centroids are given in fig. 8 as a function of $(N - Z)/A$.

Considering ^{94m1}Rh, because of the divergence of the strength owing to the high-energy part of the β-delayed proton spectrum, we estimated the energy of the SF centroid to be at the position of the high-energy peak of the GT distribution (see fig. 7). This value is also plotted in fig. 8 at the corresponding value of $(N - Z)/A$. One can see a reasonable agreement with the trend of Pd-isotopes data, which confirms the validity of an assumption about the SF character of the main maximum of the GT-strength distribution of ^{94m1}Rh.

The SF-strength distribution of ^{94m1}Rh, in its turn, consists of two components, in which the final proton configurations have seniorities $\upsilon_p = 2$ and $\upsilon_p = 0$. The configuration with $\upsilon_p = 2$ is created by the SF transformation with a proton pair breaking, in much the same as for even-even parent Pd isotopes. The $\upsilon_p = 0$ component is due to the transformation of the odd, not paired proton (see [33] for details). A calculation of Towner [33] predicted the strength with $\upsilon_p = 0$ about 0.05 of the total strength for the decay of ^{95}Rh, which can be taken as estimate for ^{94m1}Rh. Moreover, the centroid of strength with $\upsilon_p = 0$ is expected to be situated below the centroid with $\upsilon_p = 2$, therefore we can neglect a contribution of the $\upsilon_p = 0$ component in the energy region around the SF centroid. The configuration $\upsilon_p = 0$ most probably is partly responsible for the long tail of the SF strength in the excitation energy region below 7 MeV (see fig. 7).

The $E_{\rm CP}$ values of the CP-strength distributions cannot be taken directly from the experimental energies of low-lying levels because some fraction of the CP strength has to be distinguished from the low-energy wing of the strong SF-strength distribution. In particular for the ^{94m1}Rh decay, the contribution from the $\upsilon_p = 0$ component of the SF strength is possible. This distinction cannot be made on an experimental basis. In order to derive some estimate of $E_{\rm CP}$ we again turn to shell model predictions. For each of the two nuclei under consideration we calculated the energies and B(GT) values for all the levels within the $(1p_{1/2}, 0g_{9/2})$ model space. The calculations yield good agreement with experiment concerning, firstly, the excitation energies of the 1^{+}_{1} level in ^{94}Rh and the 4^{+}_{2} level in ^{94}Ru and, secondly, the feature that these levels account for the maximum fractions of the CP component of the GT strength (see also [9,10]). By using the experimental energy $E_{\rm L}$ of the 1^{+}_{1} level in ^{94}Rh and 4^{+}_{2} level in ^{94}Ru and the corresponding calculated energies $E_{\rm L,CALC}$, we estimated the $E_{\rm CP}$ values, assuming that $E_{\rm CP}$-$E_{\rm L} \approx E_{\rm CP,CALC}$-$E_{\rm L,CALC}$, with $E_{\rm CP,CALC}$ being the centroid of the GT strength calculated within the $(1p_{1/2}, 0g_{9/2})$ model space. To judge the steadiness of the results, we repeated the calculation with different interactions, namely GF [31], S-FIT [27] and F-FIT [27]. The latter was obtained by fitting more extended experimental data than those used for the GF and S-FIT interactions. In table 3, the $E_{\rm CP}$ values obtained with such corrections and $E_{\rm SF}$ values are presented. The large spread of $E_{\rm CP}$ values obtained with different interactions shows that the results obtained by this procedure represent only rough estimates. Nevertheless, the data compiled in table 3 yield evidence that the energy distances between the SF and CP states, which one may call spin-orbit splitting, differ in ^{94}Rh and ^{94}Ru by about 2 MeV.

Table 3. Values of centroids of low- and high-energy groups of GT strength related to core-polarized ($E_{\rm CP}$) and spin-flip ($E_{\rm SF}$) states.

Daughter nuclide	$E_{\rm CP}$ (MeV)			$E_{\rm SF}$ (MeV)
	GF[a]	F-FIT[a]	S-FIT[a]	
^{94}Rh	0.84	0.94	1.32	3.50(20)
^{94}Ru	3.6	3.0	3.6	7.90(20)

[a] Experimental values of $E_{\rm CP}$ corrected for the unobserved B(GT) strength using the shell model calculation with the interaction indicated by the column label (see sect. 4.2).

When comparing the properties of neighboring nuclei, it is reasonable to suggest that the pairing is responsible for such difference. All the four centroids presented in table 3 are connected with the GT transition accompanied by proton pair breaking, and both the SF transitions change the seniority of neutron final configurations at the same value. A distinction takes place for the change of the seniority of the neutron $0g_{9/2}$ orbital. It is advisable to consider the splitting between SF and CP centroids as a result of moving a neutron from the $0g_{9/2}$ to $0g_{7/2}$ orbital. In ^{94}Rh$_{49}$, a promotion of an odd neutron from the $0g_{9/2}$ orbital leads to the formation of one hole pair, and hence to a corresponding decrease in the splitting. In ^{94}Ru$_{50}$, on the contrary, the promotion of one neutron from closed shell costs more energy and leads to an increase in the splitting. Thus, the difference of the splitting is qualitatively understood in terms of the analogy with the even-odd difference of neutron separation energies and interpreting both effects as being due to pairing in the neutron $0g_{9/2}$ shell.

5 Summary and conclusion

We used heavy-ion–induced fusion-evaporation reactions, on-line mass separation and decay spectroscopy to investigate the β decays of ^{94}Pd and ^{94m1}Rh. A new isomer, ^{94m3}Rh, was identified to have a half-life of 0.48(3) μs and be de-excited by a 55 keV, $E2$ transition. Tentative spin and parity assignments of (4^{+}) and (2^{+}) were found

for ^{94m1}Rh and ^{94m3}Rh, respectively. By means of total absorption spectroscopy the β intensity distributions and $Q_{\rm EC}$ values of ^{94}Pd and ^{94m1}Rh were measured. The resulting GT-strength distributions were deduced and interpreted in comparison to shell model predictions. The case of ^{94m1}Rh is an impressive demonstration that the occurrence of the strong β decay to high-excited states makes it difficult, if not impossible, to use "apparent feedings" as obtained from the balance of γ-ray intensities. The data on β decay of nuclei with $N < 50$, *i.e.* with a partly filled neutron $g_{9/2}$ shell, are useful in theoretical studies of nuclei near ^{100}Sn. Particularly interesting is the evidence for an effect of pairing in the neutron shell that becomes apparent from the difference of the splitting of the GT strengths of neighboring nuclei. In this context, a re-investigation of the β decay of the (8^+) isomer ^{94m2}Rh and the determination of the corresponding GT strength would be of considerable interest. Moreover, a high-resolution study of the β decay of ^{94}Pd would be welcome in view of the insufficient knowledge of this decay scheme.

The authors would like to thank K. Burkard and W. Hüller for their valuable contributions to the development and operation of the GSI on-line mass separator.

References

1. E. Roeckl, Lect. Notes Phys. **651**, 223 (2004).
2. I. Mukha *et al.*, Phys. Rev. Lett. **95**, 022501 (2005).
3. I. Mukha *et al.*, Nature **439**, 298 (2006).
4. H. Schatz *et al.*, Phys. Rep. **294**, 167 (1998).
5. C. Fröhlich *et al.*, Phys. Rev. Lett. **96**, 142502 (2006).
6. G. Audi, O. Bersillon, J. Blachot, A.H. Wapstra, Nucl. Phys. A **729**, 3 (2003).
7. W. Kurcewicz *et al.*, Z. Phys. A **308**, 21 (1982).
8. K. Oxorn, B. Singh, S.K. Mark, Z. Phys. A **294**, 389 (1980).
9. I.P. Johnstone, L.D. Skouras, Phys. Rev. C **53**, 3150 (1996); **55**, 2739 (1997).
10. H. Herndl, B.A. Brown, Nucl. Phys. A **627**, 35 (1997).
11. J.C. Hardy *et al.*, Phys. Lett. B **71**, 307 (1977); J.C. Hardy, B. Jonson, P.G. Hansen, Phys. Lett. B **136**, 331 (1984).
12. M. Karny *et al.*, Nucl. Instrum. Methods Phys. Res. B **126**, 411 (1997).
13. B.A. Brown, K. Rykaczewski, Phys. Rev. C **50**, R2270 (1994).
14. Z. Hu *et al.*, Phys. Rev. C **60**, 024315 (1999); **62**, 064315 (2000).
15. M. Karny *et al.*, Nucl. Phys. A **690**, 367 (2001).
16. C. Plettner *et al.*, Phys. Rev. C **66**, 044319 (2002).
17. M. Karny *et al.*, Eur. Phys. J. A **25**, s01, 135 (2005).
18. O. Kavatsyuk *et al.*, Eur. Phys. J. A **25**, 211 (2005).
19. H.V. Klapdor, C.O. Wene, J. Phys. G **6**, 1061 (1980).
20. L. Batist *et al.*, Nucl. Phys. A **720**, 245 (2003).
21. L. Batist *et al.*, GSI Scientific Report 2003, p. 11, `http://wwwaix.gsi.de/annrep2003`.
22. B.A. Brown *et al.*, MSU-NSCL Report 1289.
23. R. Kirchner, Nucl. Instrum. Methods. Phys. Res. B **26**, 204 (1987).
24. E. Roeckl *et al.*, Nucl. Instrum. Methods Phys. Res. B **204**, 53 (2003).
25. I. Mukha *et al.*, Eur. Phys. J. A **25**, s01, 131 (2005).
26. R.S. Hager, E.C. Seltzer, Nucl. Data A **4**, 1 (1968).
27. I.P. Johnstone, L.D. Skouras, Eur. Phys. J. A **11**, 125 (2001).
28. E. Nolte, G. Korschinek, U. Heim, Z. Phys. A **298**, 191 (1980).
29. G. Audi, A.H. Wapstra, C. Thibault, Nucl. Phys. A **729**, 337 (2003).
30. J.A. Clark *et al.*, Eur. Phys. J. A **25**, s01, 629 (2005).
31. R. Gross, A. Frenkel, Nucl. Phys. A **267**, 85 (1976).
32. D. Rudolph, K.P. Lieb, H. Grawe, Nucl. Phys. A **597**, 298 (1996).
33. I.S. Towner, Nucl. Phys. A **444**, 402 (1985).
34. K. Rykaczewski *et al.*, Z. Phys. A **322**, 263 (1985).
35. K. Rykaczewski *et al.*, GSI-90-62 (1990).
36. M.S. Antony, A. Pape, J. Britz, At. Data Nucl. Data Tables **66**, 1 (1997).
37. I.P. Johnstone, Phys. Rev. C **44**, 1476 (1991).
38. A. Juodagalvis, D.J. Dean, Phys. Rev. C **72**, 024306 (2005).